JOURNAL OF COMPUTATIONAL PHYSICS **136,** 599–602 (1997)
ARTICLE NO. CP975784

White and Bird's Formulation of Gradient-Corrected Exchange-Correlation Potentials Applied to Atoms

D. M. Bylander and Leonard Kleinman

Department of Physics, University of Texas, Austin, Texas 78712
E-mail: kleinman@mail.utexas.edu

Received November 12, 1996; revised June 25, 1997

White and Bird have recently found a new way to calculate gradient corrections to the exchange-correlation potential in crystals which requires the use of fast Fourier transforms (FFT) and which for a fixed FFT mesh size has much greater numerical accuracy than the standard method. We demonstrate that FFT's can be avoided and show how the method can be applied to atoms.

Density functional theory [1] has been the mainstay of solid state electronic structure calculations for 30 years but it is only with the advent of generalized gradient approximations [2, 3] (GGA) that the method has been able to compete with the methods used by chemists for atoms and molecules. White and Bird [4] recently demonstrated a new way with important computational advantages to implement solid state GGA calculations in which the charge density is expanded in plane waves. One purpose of this paper is to introduce the method to atomic and molecular physicists who have not used it heretofore. Because the standard method of applying the GGA involves gradients of absolute values of gradients, whereas the White–Bird method (WBM) does not; for equal accuracy the standard method requires an expansion in many more basis functions (as shown below, eight times more when the basis functions are plane waves). However, the main purpose of this paper is to demonstrate how the WBM can also be applied in numerical calculations where no basis functions are used and the charge density is known only on a set of unequally spaced mesh points and, furthermore, that in this case also, the WBM is the more accurate method. For the neon atom, which will be our computational example, the density of mesh points that can be used is so large that the additional accuracy of the WBM is of no practical importance; however, when finite difference methods, involving a three-dimensional mesh, are used for large molecular calculations, the additional accuracy of the WBM will be important.

The exchange-correlation energy density functional [1] may be approximated by

$$E_{\rm xc}[n] = \int f_{\rm xc}\big(n(\mathbf{r}), |\nabla n(\mathbf{r})|\big)\, d\mathbf{r}, \tag{1}$$

where $f_{\rm xc}$ may be a complicated function of the charge density $n(\mathbf{r})$ and $|\nabla n(\mathbf{r})|$. A small variation in $n(\mathbf{r})$ results in

$$\begin{aligned}\delta E_{\rm xc} &= \int \frac{\delta E_{\rm xc}}{\delta n(\mathbf{r})}\,\delta n(\mathbf{r})\, d\mathbf{r} = \int \left[\frac{\partial f_{\rm xc}}{\partial n(\mathbf{r})}\right.\\ &\quad\left. + \int \frac{\partial f_{\rm xc}}{\partial \nabla n(\mathbf{r}')}\cdot\frac{d\nabla n(\mathbf{r}')}{dn(\mathbf{r})}\, d\mathbf{r}'\right]\delta n(\mathbf{r})\, d\mathbf{r} \qquad (2)\\ &= \int \left[\frac{\partial f_{\rm xc}}{\partial n(\mathbf{r})} - \nabla\cdot\frac{\partial f_{\rm xc}}{\partial \nabla n(\mathbf{r})}\right]\delta n(\mathbf{r})\, d\mathbf{r},\end{aligned}$$

where the last step uses an integration by parts and $dn(\mathbf{r})/dn(\mathbf{r}') = \delta(\mathbf{r} - \mathbf{r}')$. Thus the exchange-correlation potential is

$$v_{\rm xc}(\mathbf{r}) = \frac{\delta E_{\rm xc}}{\delta n(\mathbf{r})} = \frac{\partial f_{\rm xc}}{\partial n(\mathbf{r})} - \nabla\cdot\frac{\partial f_{\rm xc}}{\partial \nabla n(\mathbf{r})}. \tag{3}$$

One can see that $v_{\rm xc}$ will contain terms of the form $\nabla n\cdot\nabla|\nabla n|$. Noting that $\nabla|\nabla n| = \nabla|\nabla n|^2/2|\nabla n|$ has eight times as many reciprocal lattice vectors as n (which itself has eight times as many as the crystal wave functions are expanded in), White and Bird [4] suggested that $v_{\rm xc}$ be obtained on a finite grid using the first form of $\delta E_{\rm xc}$ in Eq. (2), i.e.,

$$\tilde{v}_{\rm xc}(\mathbf{R}) = \frac{\partial f}{\partial n(\mathbf{R})} + \sum_{\mathbf{R}'}\frac{\partial f_{\rm xc}}{\partial \nabla n(\mathbf{R}')}\cdot\frac{d\nabla n(\mathbf{R}')}{dn(\mathbf{R})}. \tag{4}$$

Writing $n(\mathbf{r})$ in terms of its Fourier transforms $n(\mathbf{G})$, they obtain

$$\nabla n(\mathbf{r}) = \sum_{\mathbf{G}} i\mathbf{G}n(\mathbf{G})e^{i\mathbf{G}\cdot\mathbf{r}} = \frac{1}{N}\sum_{\mathbf{G},\mathbf{R}} i\mathbf{G}n(\mathbf{R})e^{i\mathbf{G}\cdot(\mathbf{r}-\mathbf{R})}, \tag{5}$$

and setting $\mathbf{r} = \mathbf{R}'$ they evaluate the last term in Eq. (4) and note that $\tilde{v}_{\rm xc}$ requires no more reciprocal lattice vectors than those in which n is expanded. Equation (4) must be

0021-9991/97 $25.00

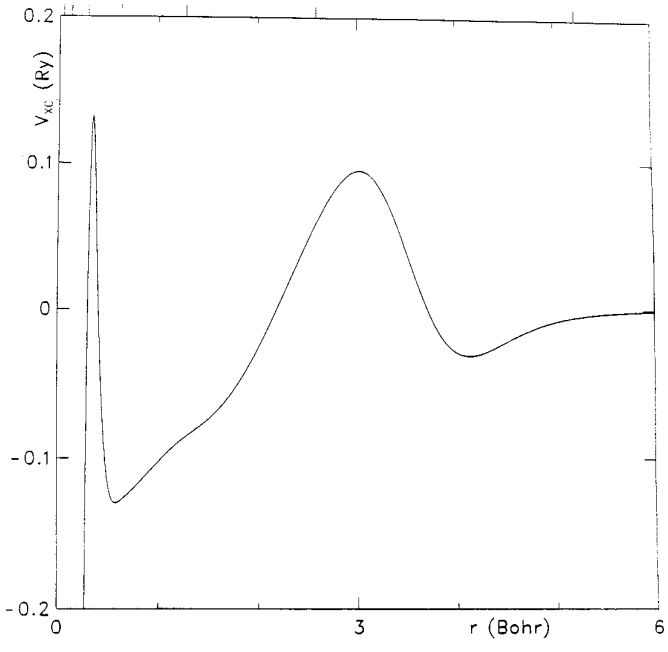

FIG. 1. The gradient term of the analytic v_{xc}.

generalized for atomic calculations to account for the fact that even if the mesh points are evenly spaced, each point represents a different volume (proportional to R^2). Write

$$E_{xc} = \sum_i f_{xc}(n(\mathbf{R}_i), \nabla n(\mathbf{R}_i))\Omega_i, \tag{6}$$

where Ω_i is the volume associated with $\mathbf{R}_i$. Then

$$\tilde{v}_{xc}(\mathbf{R}_j) = \frac{1}{\Omega_j}\frac{\delta E_{xc}}{\delta n(\mathbf{R}_j)} = \frac{\partial f_{xc}}{\partial n(\mathbf{R}_j)} + \sum_i \frac{\Omega_i}{\Omega_j}\frac{\partial f_{xc}}{\partial \nabla n(\mathbf{R}_i)}\cdot\frac{d\nabla n(\mathbf{R}_i)}{dn(\mathbf{R}_j)}. \tag{7}$$

In a crystal the sum is usually over an equally spaced lattice so that $\Omega_i/\Omega_j = 1$ and Eq. (7) reduces to Eq. (4). Note that $d\nabla n(\mathbf{r}')/dn(\mathbf{r}) = d\delta(\mathbf{r}' - \mathbf{r})/d\mathbf{r}'$. While it is obvious that, with a large enough number of $\mathbf{G}$'s in the sum, the derivative of $\nabla n(\mathbf{r})$ with respect to $n(\mathbf{R}')$ will approximate the derivative of a delta function (with an infinite number it is the derivative of a delta function), it is not at all obvious that one can, on an atomic mesh, fit $n(R_i)$ at a set of points around R_j and then sum the derivatives with respect to $n(R_j)$ of the gradients of this fit at the R_i and obtain a $\tilde{v}_{xc}(R_j)$ which is identical to $v_{xc}(R_j)$.

We use the GGA of Perdew and Wang [2] known as PW GGA II. To test the accuracy of the formulation we first fit the charge density of neon with 19 gaussians and one exponential, the latter to get a good fit to the exponential decay of $n(r)$ at small r. Then taking this analytic expression to be the charge density for which we wish to evaluate the GGA, we are able to compare $\tilde{v}_{xc}(R_i)$ and $v_{xc}(R_i)$, obtained using numerical derivatives, with the exact $v_{xc}(R_i)$ obtained analytically. We use the Herman–Skillman [5] mesh but with the points four times as dense; i.e., the minimum mesh spacing is

$$\delta = (3\pi/4)^{2/3}Z^{-1/3}/3200 = 2.568369156 \times 10^{-4}\ \text{bohr}, \tag{8}$$

where $Z = 10$ is the atomic number and the mesh spacing doubles every 160 mesh points. This will be referred to as the 4× mesh; 8× and 2× meshes will also be discussed. V_{xc}, the gradient term of the exact v_{xc} (i.e., the second term of Eq. (3)), is plotted in Fig. 1. The upward pointing tick marks along the top of the figure are the mesh doubling points. This term blows up like $-1/r$. Its values at 160 δ and at δ are -2.2371 Ry and -274.599 Ry, respectively. To numerically evaluate the first and second derivatives of n with respect to r at R_j which occur in $V_{xc}(R_j)$, we fit the charge density between R_{j-4} and R_{j+4} with the Lagrange interpolation formula [6]. However, if the mesh size doubles between those points, some points are discarded so that the remaining points occur in pairs which are equidistant from R_j.

Figure 2 is a plot of ΔV_{xc}, the difference between the numerically and analytically determined V_{xc}. The same

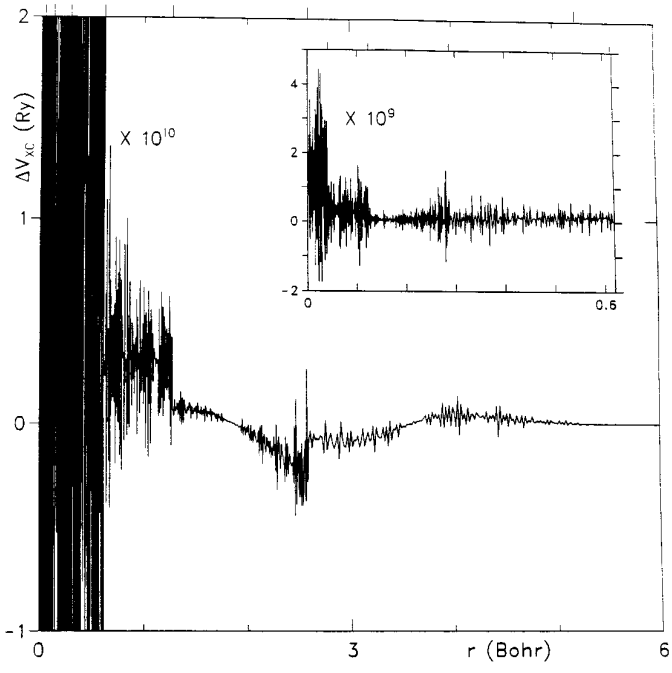

FIG. 2. The difference between the gradient terms of v_{xc} obtained with the standard numerical formulation and analytically. A nine-point interpolation scheme and the 4× mesh is used.

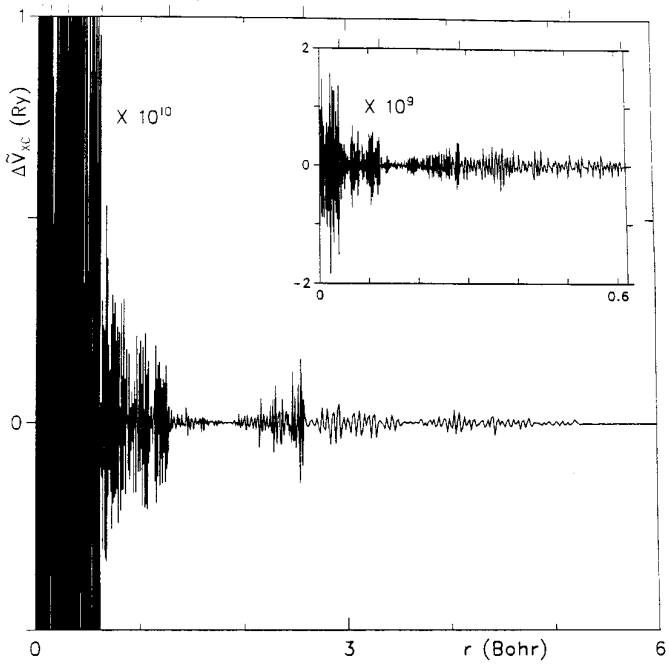

FIG. 3. The difference between the gradient terms of $\tilde{v}_x$ obtained with White and Bird's formulation and v_{xc} obtained analytically. A nine-point interpolation scheme and the 4× mesh is used.

nine-point fit is made at nine R_i around R_j to evaluate $d\nabla n(R_i)/dn(R_j)$. The fit of $n(r)$ at nine points around R_i is of the form $n(r) = \sum_{k=-4}^{4} A_k(r)n(R_{i+k})$. Thus ∇n evaluated at R_i is just $\sum_{k=-4}^{4} A'_k(R_i)n(R_{i+k})$ and the derivative with respect to $n(R_j)$ yields a $\delta_{i+k,j}$ so that $d\nabla n(R_i)/dn(R_j) = A'_{j-i}(R_i)$. The $\partial f_{xc}/\partial\nabla n(R_i)$ which multiplies this is a function of $n(R_i)$ and $\nabla n(R_i)$ and is straightforward to evaluate. One can see from the interpolation formula that this maintains the antisymmetry of the derivative of the delta function it replaces; this is the reason the R_i must be chosen to be in equidistant pairs around R_j. It is not at all obvious that the dependence of $\nabla n(R_i)$ on $n(R_j)$ more than four mesh points away can be ignored but we immediately see that it can. Figure 3 is a plot of $\Delta\tilde{V}_{xc}$, the difference between the gradient parts of $\tilde{v}_{xc}$ and the analytic v_{xc}. The first mesh point ($r = 0$), where v_{xc} and $\tilde{v}_{xc}$ are infinite is obviously not included in Figs. 2 and 3. Points 2, 3, and 4, where the fit is not made at equidistant pairs is included in ΔV_{xc} but is off-scale in the inset by an order of magnitude; $d\nabla n(R_i)/dn(R_j)$ has to be calculated with equidistant pairs. Using one pair at the second mesh point and two at the third, $\Delta\tilde{V}_{xc} = -0.198$ and -1.15×10^{-6} Ry, respectively. Not only is the numerical error represented by $\Delta\tilde{V}_{xc}$ half as large as ΔV_{xc}, over any small range of r it oscillates about zero, whereas ΔV_{xc} does not. Although these errors are completely negligible, it is clear that $\tilde{v}_{xc}$ is more numerically accurate than v_{xc}. This is because v_{xc} contains second derivatives of $n(r)$ while $\tilde{v}_{xc}$ contains only first. In principle the finer the mesh the better the nine-point fit. (The fit is, of course, exact at the nine points at which it is made; it is the interpolation between those points and, hence, the derivatives of $n(r)$ evaluated at R_j which are approximate.) But with Cray single precision, the rounding error begins to be impotant with an 8× mesh which doubles $\Delta\tilde{V}_{xc}$ and quadruples ΔV_{xc} with respect to the 4× mesh. With a 2× mesh $\Delta\tilde{V}_{xc}$ and ΔV_{xc} are both larger at large r, where the mesh is too coarse, and smaller on average at small r. Figure 4 is a plot of ΔV_{xc} with the 4× mesh but with the nine-point fit replaced by a seven-point fit. At the sixth mesh doubling point the mesh spacing becomes too large for the seven-point fit to yield accurate second derivatives of $n(r)$ and there is a large jump in ΔV_{xc} which falls off as $n(r)$ gets smoother with increasing r until the seventh mesh doubling point where another jump occurs which is much larger relative to V_{xc} than the preceding one. The effect of a seven-point mesh on $\Delta\tilde{V}_{xc}$ shown in Fig. 5 is even more dramatic. The large error beyond the sixth doubling point is due to a loss in accuracy in $d\nabla n(R_i)/dn(R_j)$. The very large glitches at the two doubling points arise from the fact that because they are multiplied by an antisymmetric function, differences occur between $\partial f_{xc}/\partial\nabla n(R_i)$ evaluated at R_i on opposite sides of and equidistant from the doubling point R_j. The errors in the first derivatives of $n(r)$ occurring in $\partial f_{xc}/\partial\nabla n(R_i)$ are still not significant, as long as they change smoothly, but around the doubling point they change rapidly because the mesh used to evaluate them is

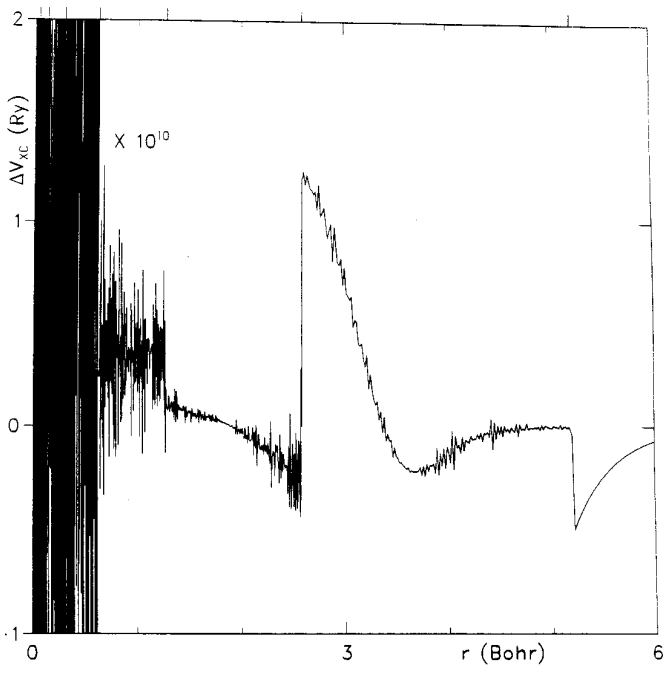

FIG. 4. Same as Fig. 2, except a seven-point interpolation scheme is used.

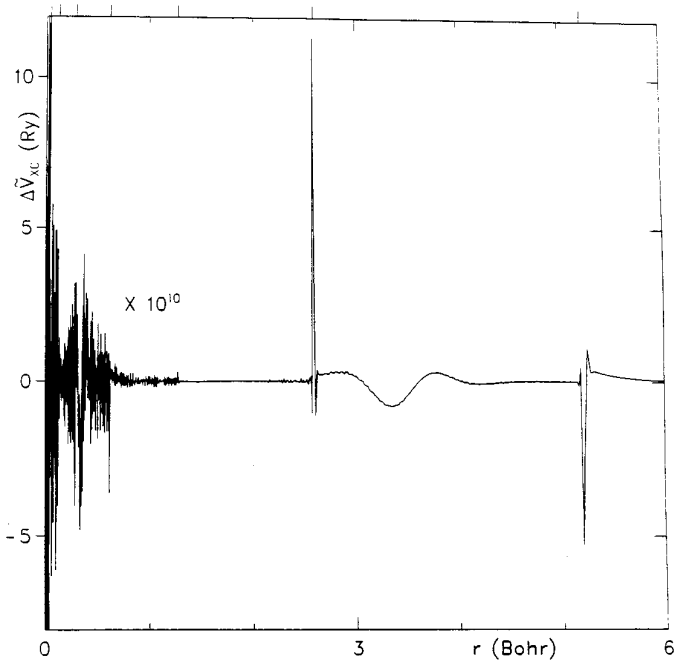

FIG. 5. Same as Fig. 3, except a seven-point interpolation scheme is used.

changing. It is this failure of the errors in the first derivative of $n(r)$ to cancel that causes the glitches.

In conclusion, we have implemented White and Bird's formulation of the GGA for atoms and shown that the numerical error incurred can be smaller than that of the standard formulation. We worked to several orders of magnitude more accuracy than normal to demonstrate that the two formulations are identical, but that their numerical errors enter in different ways.

ACKNOWLEDGMENTS

This work was supported by the University of Texas High Performance Computing Facility, the Welch Foundation (Houston, Texas) and the National Science Foundation under Grants DMR 93136745 and DMR 9614040.

REFERENCES

1. P. Hohenberg and W. Kohn, Inhomogeneous electron gas, *Phys. Rev. B* **136,** 864 (1964). [W. Kohn and L. J. Sham, Self-consistent equations including exchange and correlation effects, *Phys. Rev. A* **140,** 1133 (1965).]
2. J. P. Perdew, Unified theory of exchange and correlation beyond the local density approximation, in Electronic Structure of Solids, Vol. 91, edited by P. Ziesche and H. Eschrig (Akad. Verlag, Berlin, 1991).
3. J. P. Perdew, J. A. Chevary, S. H. Vosko, K. A. Jackson, M. R. Pederson, D. J. Singh, and C. Fiolhais, Atoms, molecules, solids, and surfaces: Applications of the generalized gradient approximation for exchange and correlation, *Phys. Rev. B* **46,** 6671 (1992).
4. J. A. White and D. M. Bird, Implementation of gradient-corrected exchange-correlation potentials in Car-Parinello total energy calculations, *Phys. Rev. B* **50,** 4954 (1994).
5. F. Herman and S. Skillman, Atomic Structure Calculations (Prentice Hall, Englewood Cliffs, NJ, 1963).
6. M. Abromowitz and Irene A. Stegun (Eds.), Handbook of Mathematical Functions, (U.S.G.P.O., Washington, 1965). [National Bureau of Standards Applied Mathematics, Ser. 55. The form given by Eqs. (25.2.6)–(25.2.7) results in less rounding error than Eqs. (25.2.1)–(25.2.2).]